

# A model for coexistent superconductivity and ferromagnetism

Jason Jackiewicz,<sup>1</sup> Krastan B. Blagoev,<sup>2</sup> and Kevin S. Bedell<sup>1</sup>

<sup>1</sup>*Department of Physics, Boston College, Chestnut Hill, MA, 02467*

<sup>2</sup>*Theoretical Division, Los Alamos National Laboratory, Los Alamos, NM, 87545*

(Dated: November 20, 2018)

We explore the various temperature dependencies and thermodynamic quantities of a mean field model of a ferromagnetic-superconducting system. The starting point for this model is based on an s-wave pairing scheme in the singlet channel of the superconducting state and a spontaneously broken symmetry phase in the ferromagnetic state. We show numerically and analytically that a state of coexistence reveals itself and is favored energetically over other possible states, and a simple phase diagram is developed. Finally, a comparison of the specific heat with experiment is shown.

PACS numbers: 71.10.-w, 71.27.+a, 75.10.LP

Much work in the past several decades has been done studying the interplay between magnetism and superconductivity. Some of the early progress by Abrikosov [1], and the work leading to the so-called LOFF model [2, 3] was directed towards ferromagnetic systems of magnetic impurities coexisting with superconducting order. Fay and Appel [4] showed how itinerant ferromagnetism can promote p-wave superconductivity, and much of the theoretical studies was concentrated on developing the symmetry of the superconducting order parameter. The question of possible s-wave singlet pairing was thought possible on the paramagnetic side of the magnetic transition, but it was shown even there that ferromagnetic fluctuations destroy it near the Curie temperature [5].

More recently, two of the current authors studied a weak ferromagnetic Fermi liquid and showed that s-wave superconductivity is possible, and that it is the favored phase on the *ferromagnetic* side [6, 7]. A possible phase diagram was predicted, however, at the time there were no materials that demonstrated superconductivity inside the ferromagnetic state. Recently a similar consideration of s-wave superconductivity has been carried out by Suhl [8] and Abrikosov [9] in which the ferromagnetism is due to localized spins. We instead develop an itinerant ferromagnetic model in which the magnetic electrons are also the ones responsible for the formation of the Cooper pairs. In this work, it must be noted that the BCS state is actually the preferred one energetically, as shown in ref.[10]. However, we are assuming that there *already exists* weak ferromagnetic order, inside which arises superconductivity. The point is that we are assuming the strongest competition to be between the coexistent and the ferromagnetic state, with the pure BCS state not being a possibility. Moreover, in the microscopic models discussed [6, 7, 8, 9], the s-wave superconductivity pairing interaction vanishes when the ferromagnetic order vanishes. With that said, we can consider this an effective mean field that has nontrivial results and can be shown to coincide with what is seen experimentally.

The phenomenon of coexistent superconductivity and ferromagnetism was then discovered in UGe<sub>2</sub> [11, 12],

and subsequently in ZrZn<sub>2</sub> [13] and URhGe [14]. The phase diagram of UGe<sub>2</sub> is very similar to the one proposed in refs.[6, 7], however, no superconductivity was detected in any of these materials on the paramagnetic side, contrary to early predictions. These current discoveries are promoting much more theoretical work to explain the superconducting pairing, with most calculations based on a p-wave triplet state [15]. Also, it has been verified [16] that the magnetic transition in at least one of these materials, UGe<sub>2</sub>, is of first-order below a certain temperature. We will not discuss the thermodynamics of that transition here, as it will be reserved for a future publication.

In this paper we will present some new and unexpected results of an alternative model of s-wave singlet pairing developed by Karchev et al.[17]. In that paper, some zero temperature results were calculated, and the finite temperature results will be shown here.

We refer the reader to ref.[17] for the details, and here we look at the mean-field Hamiltonian obtained from a model Hamiltonian by the standard mean-field procedure,

$$\begin{aligned}
 H_{mf} = & \sum_{\vec{p}} \epsilon_p (c_{\vec{p}\uparrow}^\dagger c_{\vec{p}\uparrow} + c_{\vec{p}\downarrow}^\dagger c_{\vec{p}\downarrow}) \\
 & + \frac{JM}{2} \sum_{\vec{p}} (c_{\vec{p}\uparrow}^\dagger c_{\vec{p}\uparrow} - c_{\vec{p}\downarrow}^\dagger c_{\vec{p}\downarrow}) \\
 & - \sum_{\vec{p}} (\Delta c_{\vec{p}\uparrow}^\dagger c_{-\vec{p}\downarrow}^\dagger + H.c.) + \frac{1}{2} JM^2 + \frac{|\Delta|^2}{g}. \quad (1)
 \end{aligned}$$

The diagonalization of this Hamiltonian using a Bogoliubov transformation yields,

$$H_{MF} = E_0 + \sum_{\vec{p}} \left( E_p^\alpha \alpha_{\vec{p}}^\dagger \alpha_{\vec{p}} + E_p^\beta \beta_{\vec{p}}^\dagger \beta_{\vec{p}} \right), \quad (2)$$

where

$$\begin{aligned}
 E_0 = & \sum_{\vec{p}} \epsilon_p^\downarrow + \frac{1}{2} JM^2 + \frac{|\Delta|^2}{g}, \\
 \epsilon_{\vec{p}}^{\downarrow\uparrow} = & \frac{p^2}{2m^*} - \mu \mp \frac{JM}{2}.
 \end{aligned}$$

The quasiparticle energy dispersion relations are,

$$E_p^\alpha = \frac{JM}{2} + \sqrt{\xi_p^2 + |\Delta|^2}, \quad (3)$$

$$E_p^\beta = \frac{JM}{2} - \sqrt{\xi_p^2 + |\Delta|^2}. \quad (4)$$

The final step is to minimize the free energy to produce the mean-field equations. This results in a set of two coupled equations in  $M$  and  $\Delta$  that will be solved self-consistently below. For  $M$  we find,

$$M = \frac{1}{2} \int \frac{d^3p}{(2\pi)^3} (1 - n_p^\alpha - n_p^\beta), \quad (5)$$

and for  $\Delta$ ,

$$|\Delta| = \frac{|\Delta|g}{2} \int \frac{d^3p}{(2\pi)^3} \frac{n_p^\beta - n_p^\alpha}{\sqrt{\xi_p^2 + |\Delta|^2}}. \quad (6)$$

The two order parameters,  $M$  and  $\Delta$ , have dependencies such as  $M = M(g, J)$  and  $\Delta = \Delta(g, J)$  at  $T = 0$ . From the numerical solutions of the two coupled equations (5,6), we show characteristic curves of the order parameters, a phase diagram, and the free energy difference of different states. We stress that all of the future results are derived strictly from the dispersion relations and the mean-field equations only, with no other assumptions made about coupling strength limits or small magnetization.

At  $T = 0$ , only one of the fermionic particles contributes, since  $E_p^\alpha > 0$  for all  $p$ , but  $E_p^\beta < 0$  when  $p < p_F^-$  and  $p > p_F^+$ , where

$$p_F^\pm = \sqrt{2m^*\mu \pm m^*\sqrt{(JM)^2 - 4|\Delta|^2}}. \quad (7)$$

Therefore, the coupled equations (5,6) reduce to

$$M = \frac{1}{12\pi^2} [(p_F^+)^3 - (p_F^-)^3], \quad (8)$$

and

$$|\Delta| = \frac{g|\Delta|}{2} \left[ \int_0^\infty \frac{d^3p}{(2\pi)^3} \frac{1}{\sqrt{\xi_p^2 + |\Delta|^2}} - \int_{p_F^-}^{p_F^+} \frac{d^3p}{(2\pi)^3} \frac{1}{\sqrt{\xi_p^2 + |\Delta|^2}} \right]. \quad (9)$$

The only solutions of eqs.(8) and (9) which exhibit the coexistence of superconductivity and ferromagnetism are in the case when  $JM > 2|\Delta|$ . However, in theory, there are two other solutions: the pure ferromagnetic state with  $\Delta = 0$  and the BCS state with  $M = 0$  (and obviously the normal, paramagnetic state). We will not consider the 'BCS' state here (see introduction).

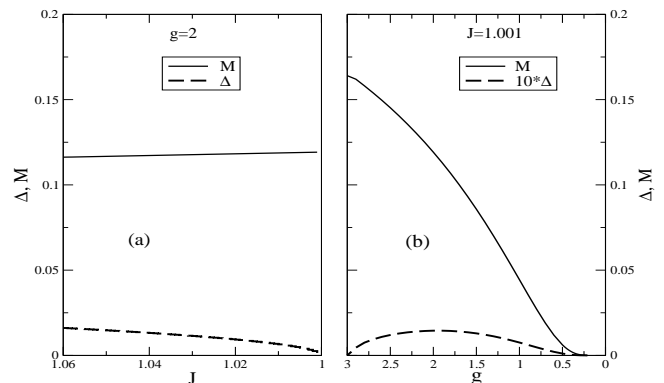


FIG. 1:  $M$  and  $\Delta$  curves at  $T = 0$  as functions of  $J$  and  $g$ . In (a) we see that these order parameters are weak functions of  $J$ , while in (b) there is strong  $g$ -dependence. Note: Here and elsewhere, by  $g$  we mean  $2\pi^2 gN(0)$ , so that these calculations are definitely in the weak-coupling regime ( $gN(0) \ll 1$ ). Also, the magnetization is normalized by  $n$ , so that  $M/n \leq 1$ .

Our concern will be with the case  $JM > 2|\Delta|$  as in ref.[17]. A note is in order here concerning the approximations made in refs.[17, 18]. Analytically, the solutions obtained from the coupled equations at  $T = 0$  when  $JM$  is close to, but larger than  $2\Delta$  are

$$I = \frac{r}{\sqrt{r^2 - 1}} \Delta, \quad \Delta = \sqrt{\frac{r-1}{r+1}} \Delta_0, \quad (10)$$

where  $\Delta_0$  is the usual energy gap equation in a non-magnetic superconducting state:

$$\Delta_0 = 2\epsilon_c \exp\left(-\frac{1}{gN(0)}\right). \quad (11)$$

The important thing to notice is that in eq.(10) the magnetization and the gap are strictly proportional to each other in the coexistent state. This is an artifact of the approximation used, and we would like to stress that the numerical calculations do not make use of this approximation. To show this explicitly, we look at Fig.1 where the coexistent solution with both order parameters is shown as a function of  $J$  and  $g$  respectively.

It is seen from this figure that both order parameters go to zero together either at  $J = 1$  or  $g = 0$ . This is due to the self-consistency of the coupled equations. As  $J$  is increased the order parameters are fairly constant and solutions can be found for large values of  $J$ . However, we are mainly interested in weak ferromagnetism, i.e., when the coupling  $J$  is close to 1, and we take the value of  $J = 1.001$ . Using this  $J$  we show the order parameters as functions of  $g$  in (b) of Fig.1. This has an interesting feature in that the superconducting gap increases from  $g = 0$  and then gets suppressed at a higher value of  $g$ . The magnetization is constant after the gap disappears because  $M$  is not an explicit function of  $g$ , only implicitly through  $\Delta$ . This feature of the gap increasing and

then being suppressed is non-existent in the approximate eqns.(10).

In Fig.2 we have calculated the free energy of the co-existent state with relation to the normal state and the pure ferromagnetic state ( $\Delta = 0$ ). In the range where the superconducting gap has its largest value,  $g \approx 2$  (see Fig.1b), the free energy of the superconducting ferromagnetic state is lower than the two other states, and hence is the preferred one. For very small values of  $g$ , we see a crossover. This behavior will also be evident in the finite temperature free energy, where the area around the largest value for  $T_c$  in the superconducting state yields a lower free energy.

At finite temperatures one can look at the same types of dependencies of the order parameters. We solve eqtns.(5,6) introducing a debye cutoff in the otherwise divergent integrals. The cutoff is small compared to the Fermi energy as this is the region where the important physics takes place, and varying this cutoff has no qualitative effects on the various quantities calculated below. A phase diagram can also be developed which shows how the  $T_c$ 's depend on the coupling constants. Then, thermodynamic properties can be calculated such as the free energy and specific heat.

The temperature dependence of  $M$  and  $\Delta$  can differ widely with respect to changes in the coupling constant space. This is why this model is convenient because it is adaptable for different cases. By tuning the parameters we can see physically realizable results. Figure 3 shows some examples. In (a),  $g = 0$  and we see the full magnetization as it approaches its Curie temperature. There is no superconducting gap in this case. In the second and third graphs, we now turn on the superconducting coupling and see that it has dramatic effects on the magnetization. There are two cases. For a small  $g$ , the  $T_c$  for  $M$  and  $\Delta$  coincide. The superconductivity weakens the magnetization and they become proportional and si-

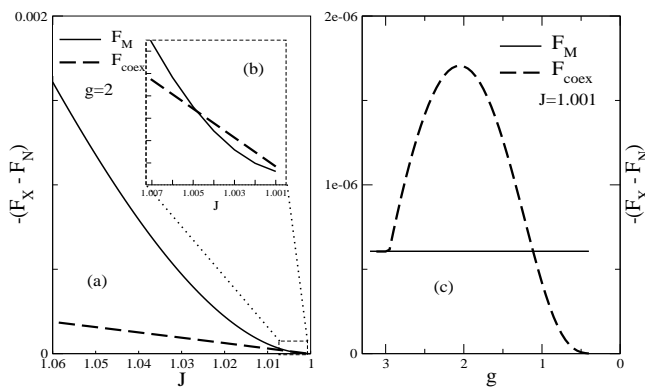


FIG. 2: Free energy of various states with respect to the normal state ( $\Delta = M = 0$ ). Notice where the coexistent state has its lowest free energy value (see Fig.1), i.e., where the gap has its largest value.

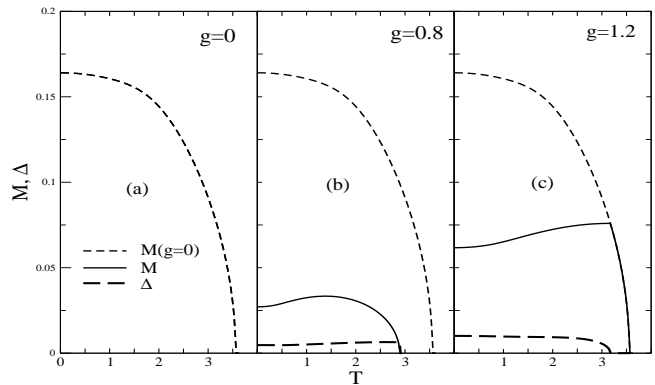


FIG. 3: The temperature dependence of the order parameters for different coupling values of  $g$ . Here,  $J = 1.001$ . The temperature,  $T$ , is unitless, but can be converted to Kelvin with one input parameter, the Fermi energy. For example, using this conversion for  $UGe_2$ , the approximate temperature is  $\approx 5T$ [K]. This gives a Curie temperature of the right order of magnitude.

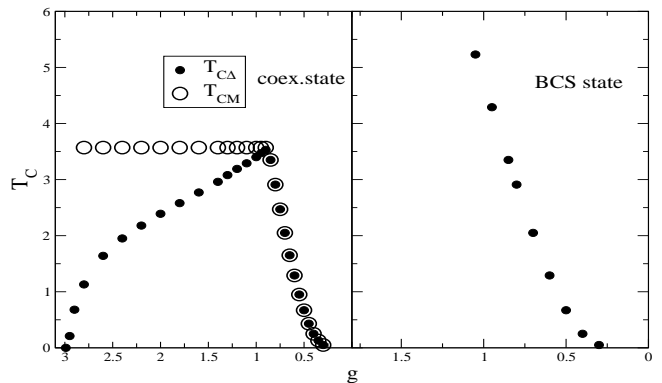


FIG. 4: A typical phase diagram for a fixed value of  $J=1.001$  with the  $T_c$ 's on the y-axis. Also shown for comparison is the  $T_c$  dependence of a pure BCS superconductor on  $g$ .

multaneously go to zero. The second case is for a larger  $g$  where now the  $T_c$ 's differ. The gap disappears and the magnetization falls back onto the full saturation curve, as expected from the equations.

In Fig.4 a phase diagram is developed from this model. It shows the  $T_c$ 's of each order parameter of the co-existent solution plotted as functions of  $g$ . In (b) is the phase diagram of a normal BCS superconductor without magnetic ordering and in comparison with (a), it is obvious that the effect of the magnetization as it gets large is to suppress and then kill superconductivity. The superconducting  $T_c$  goes through a maximum and then is suppressed eventually to zero.

As with the zero temperature case, the free energy of the coexistent state is lower than that of the pure ferromagnetic state through a broad temperature range for certain values of the coupling constants. In Fig.5 we show one case. This particular plot is calculated with  $g = 1.2$ ,

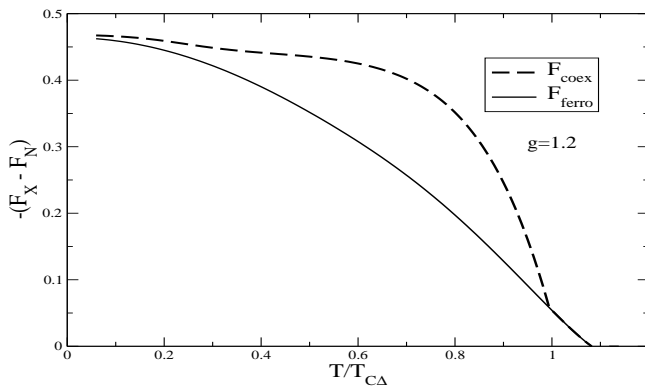


FIG. 5: The y-axis is labelled as the negative of the free energy difference of a certain state and the normal state, in arbitrary units.  $T = T_{c\Delta}$  where the superconducting gap parameter vanishes inside the magnetic state, at the point where the coexistent  $\rightarrow$  ferromagnetic transition is. The dashed curve does merge smoothly yet abruptly with the solid curve, at which point the two lines become indistinguishable.

hence it is helpful to refer to Fig.4(a) to see which part of the phase diagram we are analyzing. In this case, we are looking at the zone where the  $T_c$ 's of the two order parameters do not coincide.

Experiments have indicated that the specific heat displays a very small jump ( $UGe_2$ )[19] or an undetectable one ( $ZrZn_2$ )[13]. It also shows a very linear temperature dependence at low T. This is significant in our model because small jumps can be explained by gaplessness, which we have with the  $\beta$ -fermion. Analytically, the specific heat jump can be calculated readily to give,

$$\Delta C = \frac{\beta}{T} \frac{d\Delta^2}{d\beta} N(0) \left[ 1 + \frac{\beta}{16} JM \int \frac{d\varepsilon}{\varepsilon} \left[ \operatorname{sech}^2 \frac{\beta}{2} \left( \frac{JM}{2} + \varepsilon \right) - \operatorname{sech}^2 \frac{\beta}{2} \left( \frac{JM}{2} - \varepsilon \right) \right] \right]. \quad (12)$$

The first term on the right gives the usual BCS specific heat jump, however the remaining quantity, which is negative, gives the decrease from the BCS value. Thus, the jump can be tuned depending on the value of the magnetization. In Fig.6 is the numerical plot of the specific heat jump at the superconducting transition inside the coexistent state. The specific heat is calculated with a value of  $g = 1.1$  which corresponds to 'strong' superconductivity, i.e., where  $T_{c\Delta}$  is large. This can be seen in the phase diagram, Fig.4. Also shown for comparison are some experimental data points for  $UGe_2$  and it is clear that the numerical calculations model well the qualitative behavior of the specific heat. In that experiment, ref.[19], the specific heat is measured at 1.13 GPa where superconductivity is maximum.

In this paper, a mean field solution of s-wave pairing was investigated and shown to give nontrivial results and can be the starting point for more detailed calculations

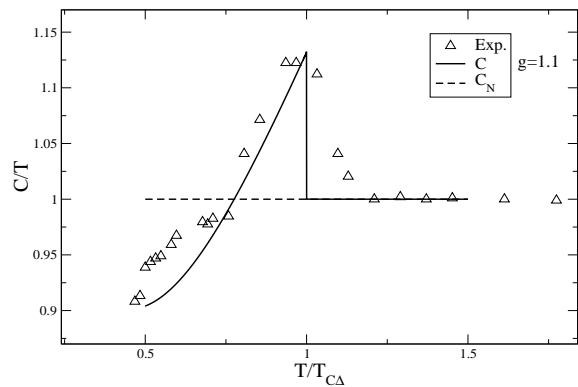


FIG. 6: The specific heat jump is much smaller than the BCS one, in this case about 15 percent. The (rescaled) experimental data is taken from ref.[19]

beyond mean field. It is important to realize that the question of the nature of the superconducting order parameter is still an open one, and we show that a model of s-wave pairing is at least qualitatively viable.

We graciously thank J.R. Engelbrecht, Y. Joglekar, N.I. Karchev, A.G. Lebed, and P.B. Littlewood for useful discussions. This work was done with the support of DOE Grants No. DEFG0297ER45636 and No. 60202ER63404.

- 
- [1] A. A. Abrikosov, *Fundamentals of the Theory of Metals* (North Holland, New York, 1988).
  - [2] A. Larkin and Y. N. Ovchinnikov, Zh. Eksp. Teor. Fiz. **47**, 1136 (1964).
  - [3] P. Fulde and R. Ferrell, Phys. Rev. **135**, A550 (1964).
  - [4] D. Fay and J. Appel, Phys. Rev. B **22**, 3173 (1980).
  - [5] N. Berk and J. Schrieffer, Phys. Rev. Lett. **17**, 433 (1966).
  - [6] K. Blagoev, J. Engelbrecht, and K. Bedell, Phil. Mag. Lett. **78**, 169 (1998).
  - [7] K. Blagoev, J. Engelbrecht, and K. Bedell, Phys. Rev. Lett. **82**, 133 (1999).
  - [8] H. Suhl, Phys. Rev. Lett. **87**, 167007 (2001).
  - [9] A. Abrikosov, J. Phys. Cond. Matt. **13**, L943 (2001).
  - [10] X. Lei, C. Ting, and J. Birman, Phys. Rev. B **29**, 2483 (1984).
  - [11] S. Saxena, P. Argarwal, K. Ahllan, F. Grosche, R. Haselwimmer, M. Steiner, E. Pugh, I. Walker, S. Julian, P. Monthoux, et al., Nature **406**, 587 (2000).
  - [12] E. Bauer, R. Dickey, V. Zapf, and M. Maple, J. Phys. Cond. Matt. **13**, L759 (2001).
  - [13] C. Pfleiderer, M. Uhlarz, S. Hayden, R. Vollmer, H. Lohneysen, N. Bernhoeft, and G. Lonzarich, Nature (London) **412**, 58 (2001).
  - [14] D. Aoki, A. Huxley, E. Ressouche, D. Braitwaite, J. Flouquet, J.-P. Brison, E. Lhotel, and C. Paulsen, Nature (London) **413**, 613 (2001).
  - [15] Z. Wang, W. Mao, and K. Bedell, Phys. Rev. Lett. **87**,

- 257001 (2001).
- [16] C. Pfeleiderer and A. Huxley, Phys. Rev. Lett. **89**, 147005 (2002).
- [17] N. Karchev, K. Blagoev, K. Bedell, and P. Littlewood, Phys. Rev. Lett. **86**, 846 (2001).
- [18] R. Shen, Z. Zheng, S. Liu, and D. Xing, cond-  
mat/0206418.
- [19] N. Tateiwa, T. Kobayashi, K. Hanazono, K. Amaya, Y. Haga, R. Settai, and Y. Onuki, J. Phys. Cond. Matt. **13**, L17 (2001).